Research Article

Properties of Surface Plasmon Polaritons Excited by Higher-Order Radially Polarized Laser Beams

R. Murugesan[1], N. Pasupathy[1], K. B. Rajesh[2*], M. Udhayakumar[2], K. Prabakaran[3]

[1]Department of Electronics, Erode Arts and Science College, Erode, TN, India
[2]Department of Physics, Chikkana Government Arts College, Tiruppur, TN, India
[3]Department of Physics, Mahendra Arts and Science College (Autonomous), Namakkal, TN, India
*rajeskb@gmail.com

ABSTRACT

Properties of surface Plasmon polaritons (SPPs) excited by generalized radially polarized higher-order transverse mode beam in high-numerical-aperture microscopic system is investigated theoretically based on vector diffraction theory. A variety of total field distributions such as virtual probe, flat-topped pattern, and doughnut can dynamically be obtained through properly selecting suitable transverse mode and pupil to beam ratio of different mode beams.

Keywords: Higher-Order radially polarized beam; Surface Plasmon Polaritons (SPPs); Vector diffraction theory.

1. INTRODUCTION

A surface plasmon polarations (SPP) is a surface electromagnetic wave, whose electromagnetic field is confined to the near vicinity of the dielectric–metal interface. This confinement leads to an enhancement of the electromagnetic field at the interface, resulting in an extraordinary sensitivity of SPPs to surface conditions. This sensitivity is extensively used for studying adsorbents on a surface, surface roughness, and related phenomena. Surface plasmon polariton-based devices exploiting this sensitivity are widely used in chemo and bio-sensors (Homola *et al.* 1999). The enhancement of the electromagnetic field at the interface is responsible for surface-enhanced optical phenomena such as Raman scattering, second harmonic generation (SHG), fluorescence, etc. (Anatoly Zayats *et al.* 2005). SPP also enable focusing into highly confined spots with sizes significantly beyond the diffraction limit. Depending on the material and frequency range SPPs possess much shorter effective wavelengths and their fields are strongly confined to the surface rather than being focused in free-space. By structuring a conductive surface on which the SPPs are generated their propagation can be efficiently manipulated, enabling guiding or lensing functionality. Circular geometries allow focusing the plasmonic field in the center of the structure, where they form a sharp frequency-dependent focal spot well described by a zero-order Bessel function (Chen and Zhan, 2009; Gilad *et al.* 2009). Naturally, radially polarized light is a better choice than linearly polarized light for the illumination of such a circular plasmonic lens, since it is always TM polarized .Moreover,in this case SPPs are launched in-phase forming a homogeneous plasmon focus through

constructive interference of the counter-propagating surface plasmon waves. As a result, radially polarized illumination gives rise to orders of magnitude larger enhancements of the field at the focus of the plasmonic lens than when illuminated by conventional linearly polarized light. More interestingly, the plasmonic focus generated this way forms an evanescent non-spreading Bessel beam (Qiwen Zhan *et al.* 2006; Hu *et al.* 2010; Wenjun Gu *et al.* 2011; Tan *et al.* 2008). A higher-order radially polarized modes with multi-ring beam patterns that are expressed as R-TEMp1* are also rotationally symmetric and have $p+1$ rings (where p is the radial mode number). The lowest-order R-TEM01* mode can be generated from a laser cavity (Hamazaki *et al.* 2008) and higher-order radially polarized R-TEMp1* modes can be generally produced by using a polarization-selective optical element or mechanism (Moser *et al.* 2005; Kozawa *et al.* 2005). The focusing of a higher-order radially polarized mode beam (Kozawa *et al.* 2006) such as an R-TEM11* is similar to the superresolution techniques that require a complex annular pupil or phase mask in imaging systems (Quabis *et al.* 2000; Helseth *et al.* 2004; Sheppard, 2004). Kosava *et al.* studied the intensity distributions near the focal point for radially polarized laser beams including higher-order transverse modes are calculated based on vector diffraction theory (kozava *et al.* 2007). They reported that double-ring-shaped radially polarized mode R-TEM11* beams can effectively reduce the focal spot size because of destructive interference between the inner and the outer rings with π phase shift .Yaoju Zhang et.al., reported that two higher-order radially polarized modes of R-TEM11* and R-TEM21* are useful to near-field optical recording (Zhang *et al.* 2009). Recently lot of work has been devoted to study the focusing properties of higher

order radially polarized beam (Moser *et al.* 2005; Rajesh *et al.* 2011; Lalithambigai *et al.* 2013). To best of our knowledge there are no studies till done on the excitation of SPP by higher order RPB. In this paper we study the SPP excited by higher order RPB using the Krectschmann-Raether configuration. We describe the higher order RPB and then the mathematical expression of excited SPP field near the metal surface using the vector diffraction theory.

2. THEORY

The proposed setup is shown in fig. 1. A radially polarized beam illuminating the pupil plane of an aplanatic lens (NA=1.49) produces a spherical wave converging toward a dielectric–metal interface located at the focal plane. A oil immersion material is used to match the index of refraction of the dielectric substrate. In this paper, the refractive indices of the thin metal film and the glass substrate and air are chosen to be $n_2 = (-10.2 + 0.82381)^2, n_1 = 1.516, n_3 = 1$. A wavelength of source is choosen as 532nm. For the strongly focused radially polarized illumination, the entire beam is *p*-polarized with respect to this multilayer interface.
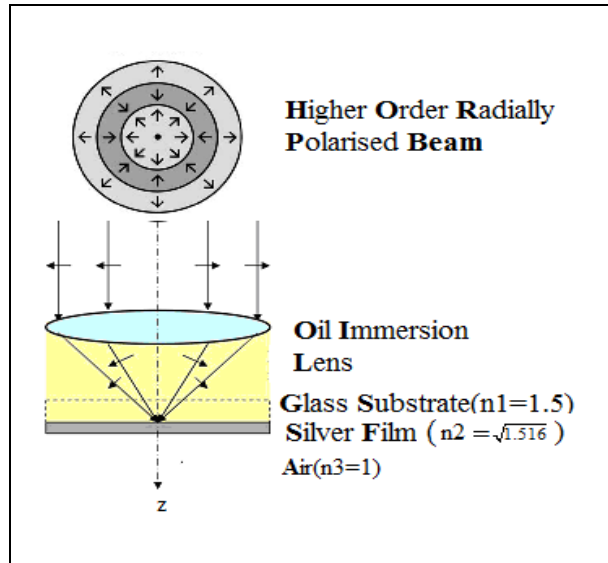

Fig. 1: Optical setup for SPPs excitation by means of an oil-immersion objective lens with a high NA for the radially polarized beam for $\varphi o = 0$

Mathematically, the electric field of the generalized CV beam can be described as (Zhan, 2009):

$$E(r,\varphi,z) = F(r,0)[\cos(\varphi + \varphi o)\hat{e}_x + \sin(\varphi + \varphi o)\hat{e}_y] \rightarrow (1)$$

where r and ϕ are the polar coordinates , F is a relative amplitude, φo is the deviation angle from the radial direction of each point of the field vector at a particular

location in the beam cross section, and $\hat{e}_x, \hat{e}_y$ are the unit vectors along x and y axis, respectively.

The electric field distributions of the excited SPPs on the metal film can be calculated with the Richard–Wolf vector diffraction theory (Richards and Wolf, 1959). When the CVB is focused by a high NA objective, the field components in the air are derived in cylindrical coordinates (rs, ϕs, zs) as (Zhongsheng Man *et al.* 2015).

$$E_r(r_s,\varphi_s,z_s) = \frac{-iB}{\pi}\int_0^{2\pi}\int_0^{\alpha}\sin\theta P(\theta)A(\theta)\times$$
$$\exp\left\{i\left[r_s k_1\sin\theta\cos(\varphi-\varphi_s) + z_s\sqrt{k_3^2 - k_1^2\sin^2\theta}\right]\right\}$$
$$\times[\sin\varphi_o\sin(\varphi_s-\varphi) + \cos\varphi_o\cos\theta\cos(\varphi-\varphi_s)]t_p^r(\theta)\,d\varphi\,d\theta \rightarrow (2)$$

$$E_\psi(r_s,\varphi_s,z_s) = \frac{-iB}{\pi}\int_0^{2\pi}\int_0^{\alpha}\sin\theta P(\theta)A(\theta)\times$$
$$\exp\left\{i\left[r_s k_1\sin\theta\cos(\varphi-\varphi_s) + z_s\sqrt{k_3^2 - k_1^2\sin^2\theta}\right]\right\}$$
$$\times[\sin\varphi_o\cos(\varphi_s-\varphi) + \cos\varphi_o\cos\theta\sin(\varphi-\varphi_s)]t_s(\theta)\,d\varphi\,d\theta \rightarrow (3)$$

$$E_z(r_s,\varphi_s,z_s) = \frac{-iB}{\pi}\int_0^{2\pi}\int_0^{\alpha}\sin\theta P(\theta)A(\theta)$$
$$\times\exp\left\{i\left[r_s k_1\sin\theta\cos(\varphi-\varphi_s) + z_s\sqrt{k_3^2 - k_1^2\sin^2\theta}\right]\right\}$$
$$\times(-\sin\theta\cos\varphi_o)t_p^z(\theta)\,d\varphi\,d\theta \rightarrow (4)$$

where θ and ϕ denote the tangential angle with respect to the z-axis and the azimuthal angle with respect to the x-axis respectively; φ_o is the deviation angle from the radial direction of the field vector in the beam cross section and for the radially polarized beam $\varphi_o = 0$. α is the convergence semi-angle of the lens; $P(\theta)$ is the pupil function of the input beam and $A(\theta)$ is the apodization factor of the focusing lens. Here k_1 and k_3 are the wave number in the glass substrate and air, respectively; and t_p^r, t_p^z and t_s are the transmission coefficients of E_r, E_ϕ, and E_z components through the metal film at incident angle of θ.

The transmission efficiencies can be derived as follows:

$$t_p^r = \frac{\sqrt{(\varepsilon_3 - \varepsilon_1)\sin^2\theta}}{\cos\theta} \times \frac{t_p^{12}t_p^{23}\exp(ik_{2z}d)}{1 - r_p^{12}r_p^{23}\exp(i2k_{2z}d)} \rightarrow (5)$$

$$t_s = \frac{t_s^{12}t_s^{23}\exp(ik_{2z}d)}{1 - r_s^{12}r_s^{23}\exp(i2k_{2z}d)} \rightarrow (6)$$

$$t_p^z = \frac{\sqrt{\varepsilon_1}}{\sqrt{\varepsilon_3}} \times \frac{t_p^{12}t_p^{23}\exp(ik_{2z}d)}{1 - r_p^{12}r_p^{23}\exp(i2k_{2z}d)} \rightarrow (7)$$

k_{2z} denotes the z-component of wave vector within the metal film, and d is the metal film thickness, respectively. t_s^{ij} and t_p^{ij} are the Fresnel transmission coefficients for s- and p-polarization at the i/j interface, r_s^{ij} and r_p^{ij} the corresponding reflection coefficients (Zhang, 2008).

$$t_s^{ij} = \frac{2\sin\theta_j\cos_i}{\sin(\theta_i + \theta_j)} \longrightarrow (9)$$

$$t_p^{ij} = \frac{2\sin\theta_j\cos_i}{\sin(\theta_i + \theta_j)\cos(\theta_i - \theta_j)} \longrightarrow (10)$$

$$r_s^{ij} = 1 - t_s^{ij} \longrightarrow (11)$$

$$r_p^{ij} = 1 - t_p^{ij} \longrightarrow (12)$$

The pupil function for the double ring shaped beam can be expressed as (Kozawa, et al. 2007)

$$P(\theta) = \frac{\beta_O^2 \sin(\theta)}{\sin^2\alpha} \exp\left(-\frac{\beta_O^2 \sin^2(\theta)}{\sin^2\alpha}\right) L_p^1\left(2\frac{\beta_O^2 \sin^2(\theta)}{\sin^2\alpha}\right) \longrightarrow (8)$$

where β is the ratio of the pupil radius and the beam waist and L_p^1 is the generalized Laguerr polynomial. The fig. 2 shows the transmission coefficient curve versus incident angle for the three layer interfaces. It is observed from the figure as if in reference (Zhongsheng Man et al. 2015) the strong longitudinal and radial component exhibits a sharp peak at $\varphi_o = 43.8^0$ showing that the beams are able to excite SPPs.

3. RESULTS & DISCUSSION

3.1 Smallest Spot and Extended Depth

The effect of pupil to beam ratio of the incident higher order radially polarized beam on the generated plasmonic focal structure is shown in figure(3). Initially the value of pupil to beam ratio (β) of each mode are assumed to be 1.6. It is observed from the figure 3.(a), the FWHM of the generated focal spot are measured to be 0.4548λ, 0.4211λ, 0.7632λ, 0.5414λ, 0.5226λ for the radial mode number P=0,1,2,3 and 5 respectively. Figure 3(b) shows the corresponding on axial intensity. The Depth of focus is considered as FWHM of the on axial intensity and are found to be 0.1805λ,0.1547λ,0.3609λ,0.2613λ,0.2368λ corresponding to the radial mode number P=0, 1, 2, 3 and 5 respectively.
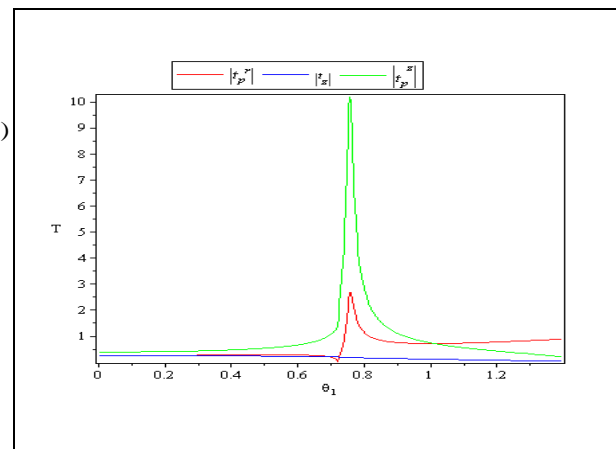

Fig. 2: Calculated amplitude transmission coefficient for the radially, azimuthally and longitudinally polarized components of the light incident on the substrate/metal interface. The surface plasmon resonance angle is satisfied at about 43.8°
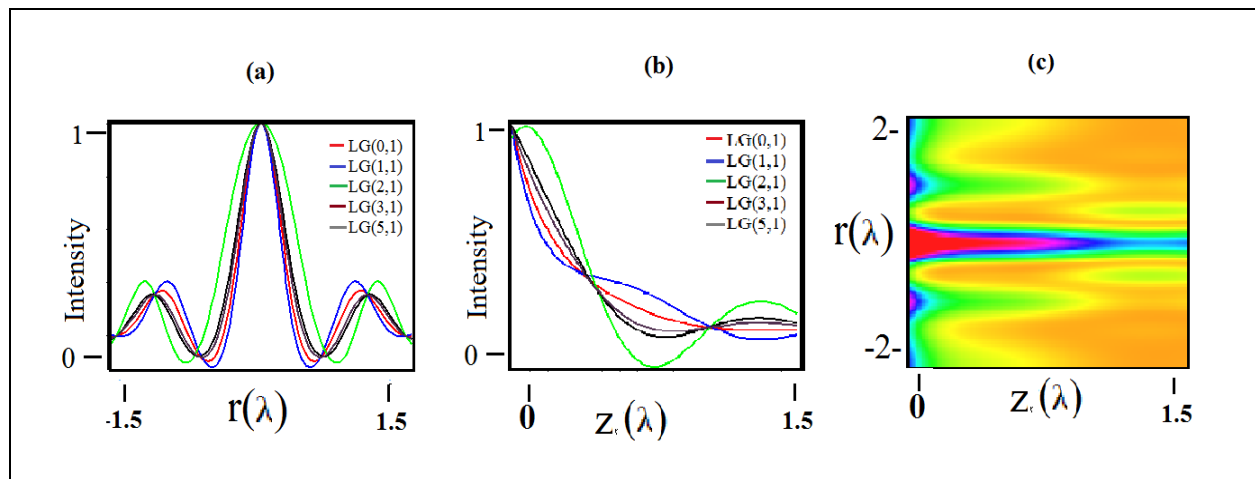

Fig. 3 (a & b): 2d intensity profiles in transverse and longitudinal direction for R-TEM01* R-TEM11*, R-TEM21*, R-TEM31*, R-TEM51* modes. (c) 3d intensity distribution for R-TEM11* mode with β=1.6. The parameters for calculation are NA=1.49, λ=532nm,d=48nm. The FWHM of the focal spot as 0.4211λ and focal depth is measured as 0.1547λ

Thus from the figures the smallest focal spot is obtained for R-TEM (1, 1)* mode and the largest focal depth is obtained for the radial mode with R-TEM (2, 1)*. It is also observed that further increasing of β to 2, R-TEM (1, 1)* mode produced a smallest focal spot of 0.42λ with focal depth of 0.206λ and are shown in fig (4).It is also observed that when β increased to 2.4, R-TEM(3,1)* generates a smallest focal spot with FWHM of 0.42λ and focal depth of 0.76λ and are shown in fig.(5).Thus by properly tuning the pupil to beam ratio and selecting suitable radial mode a highly confined plasmonic field with large focal depth can be achieved.
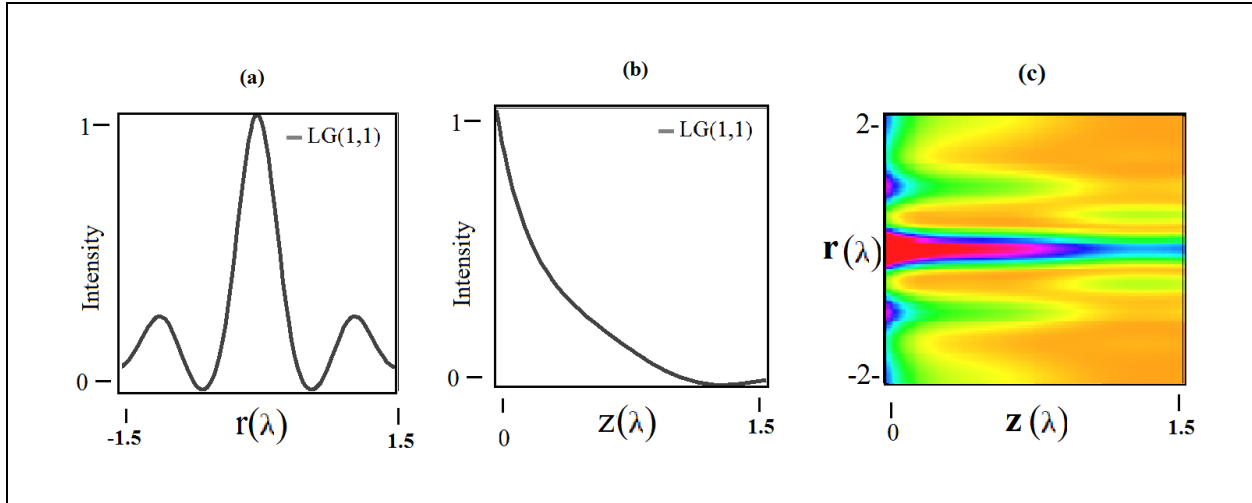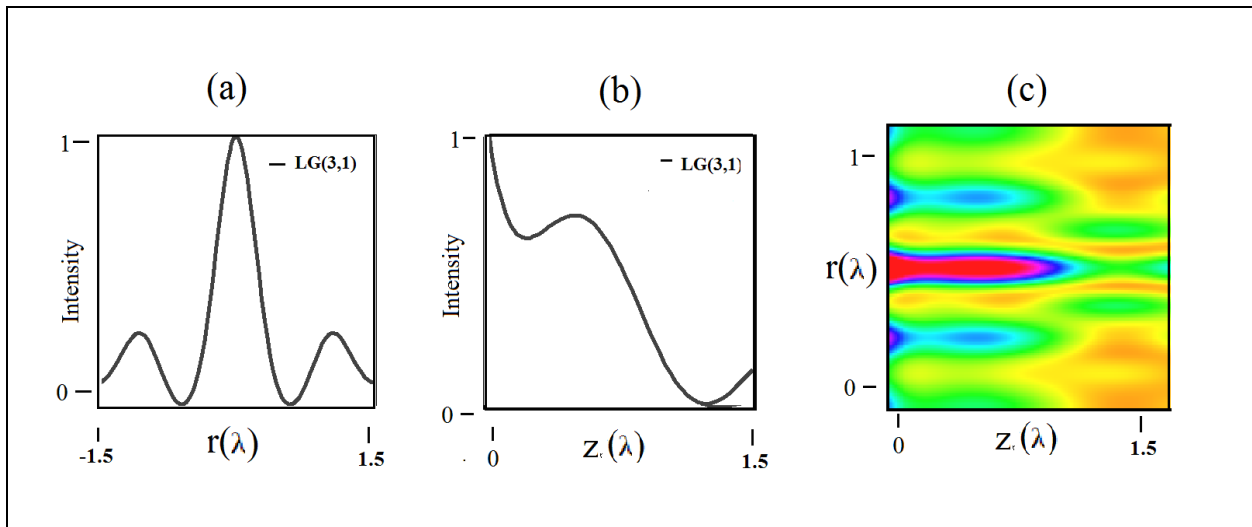

Fig. 4. (a & b): 2d intensity profiles in transverse and longitudinal direction for R-TEM11 * mode. (c) 3d intensity distribution for R-TEM11 * mode with β=2. The parameters for calculation are NA=1.49, λ = 532nm, d = 48nm. The FWHM of the focal spot as 0.4211λ and focal depth is measured as 0.2068 λ

Fig. 5 (a & b): 2d intensity profiles in transverse and longitudinal direction for R-TEM31 * mode. (C) 3d intensity distribution for R-TEM31 * mode with β=2.4

3.2 Flat Top Profile

On the attempt to achieve flat top profile we observed that by setting β to 1.64, R-TEM(2,1)* mode beam generates a flat top profile structure as shown in fig 6. The fig 6(a) shows the FWHM of the focal spot as 0.935λ and from the fig .6(b) focal depth is measured as 0.40λ.

Further it is observed that R-TEM(3,1)* mode beam also generates flat top profile corresponding to β 1.926. The FWHM of focal structure is measured as 0.98λ and focal depth as 0.38λ and are shown in fig.(7). It is also noted that when β increased to 2.445, R-TEM (5,1)* mode beam generated a flat top profile beam with FWHM of 1.14λ and focal depth of (0.357λ) as shown in fig.(8).

3.3 Focal Hole

It is observed from fig.(9), when β =3.4, R-TEM(5,1)* gives a focal hole with FWHM of 0.62λ and focal depth as 1.4λ. Thus by using higher order modes and by properly tuning the pupil to beam ratio many novel focal plasmonic structures such as much confined focal spot with extended focal depth, flat top focal structure and focal hole are generated. Such a focal patterns are use full near field application.
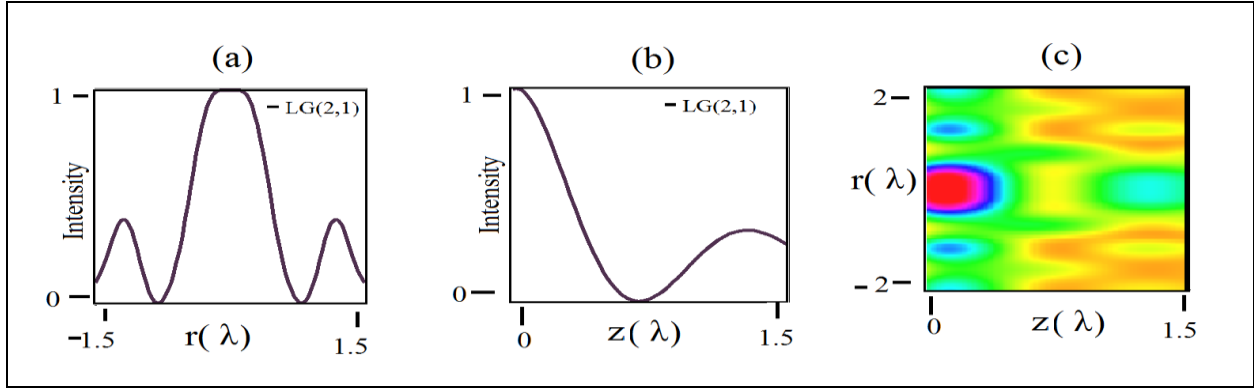

Fig. 6(a & b): 2d intensity profiles in transverse and longitudinal direction for R-TEM21 * mode. c 3d intensity distribution for R-TEM21 * mode with β=1.634
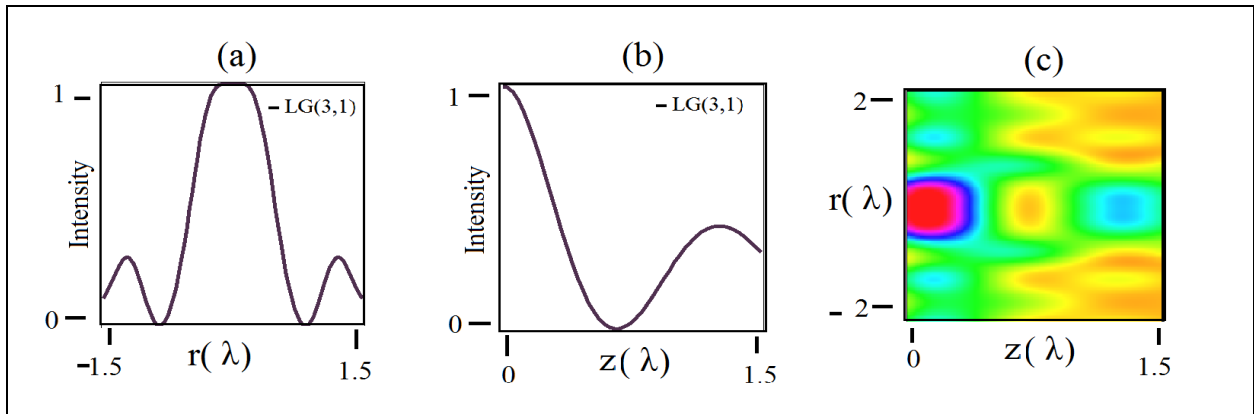

Fig. 7(a & b): 2d intensity profiles in transverse and longitudinal direction for R-TEM31 * mode. (c) 3d intensity distribution for R-TEM31 * mode with β=1.926
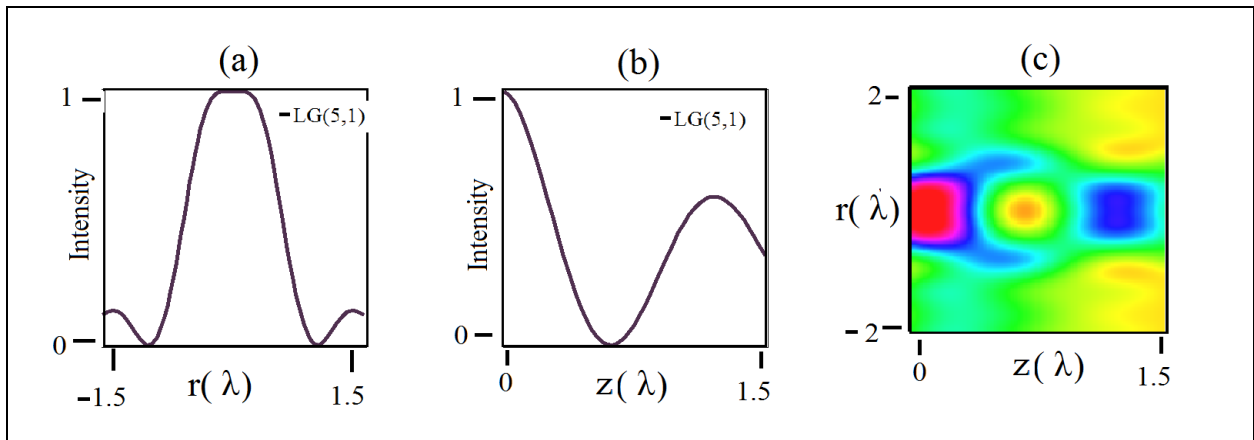

Fig. 8 (a & b) 2d intensity profiles in transverse and longitudinal direction for R-TEM51 * mode. c 3d intensity distribution for R-TEM51 * mode with β=2.445
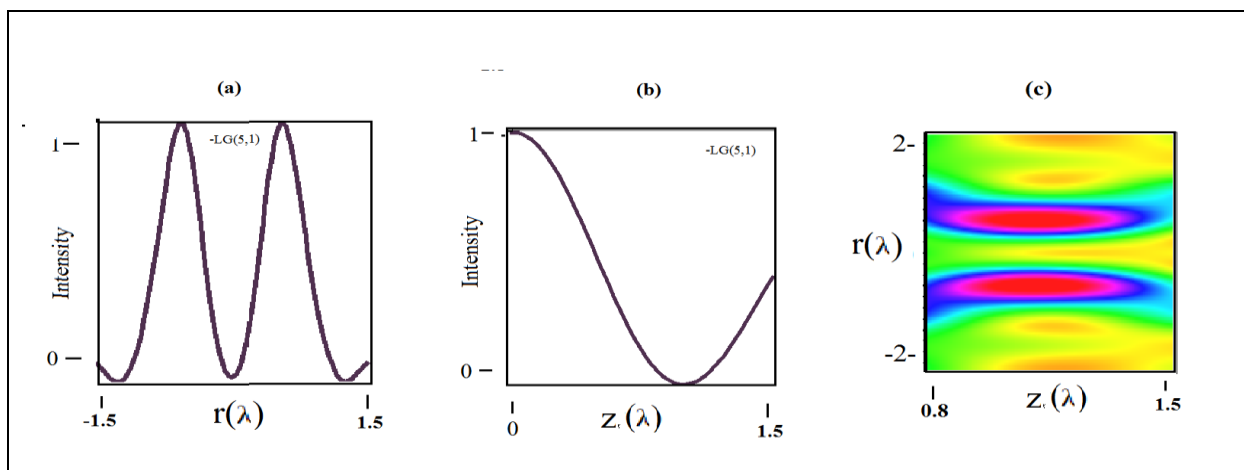
Fig. 9(a & b): 2d intensity profiles in transverse and longitudinal direction for R-TEM51 * mode. b 3d intensity distribution for R-TEM51 * mode with β=3.4

4. CONCLUSION

The intensity distributions near the focal point for radially polarized laser beams including higher-order transverse modes are calculated based on vector diffraction theory.It is observed total field distributions such as virtual probe, flat-topped pattern, and doughnut can dynamically be obtained through properly selecting suitable transverse mode and pupil to beam ratio of different mode beams.

FUNDING

This research received no specific grant from any funding agency in the public, commercial, or not-for-profit sectors.

CONFLICTS OF INTEREST

The authors declare that there is no conflict of interest.

COPYRIGHT

REFERENCE

Anatoly Zayats, V., Igor, I. Smolyaninov and Alexei A. Maradudin, Nano-optics of surface plasmon polaritons, *Phys. Rep.,* 408, 131-314(2005).
https://doi.org/10.1016/j.physrep.2004.11.001

Bouhelier, A., Ignatovich, F., Bruyant, A., Huang, C., Colas des Francs, G., Weeber, J. C., Dereux, A. Wiederrecht, G. P. and Novotny, L., Surface plasmon interference excited by tightly focused laser beams, *Opt. Lett.,* 32, 2535-2537(2007).
https://doi.org/10.1364/ol.32.002535

Chen, W., Abeysinghe, D. C., Nelson, R. L. and Zhan, Q., Plasmonic lens made of multiple concentric metallic rings under radially polarized light, *Nano Lett.,* 9, 4320-4325(2009).
https://doi.org/10.1021/nl903145p

Chen, W. B. and Zhan, Q., Realization of an evanescent Bessel beam via surface plasmon interference excited by a radially polarized beam, *Opt. Lett.,* 34(6), 722-724(2009).
https://doi.org/10.1364/ol.34.000722

Gilad, M. Lerman., Yanai, A. and Levy, U., Demonstration of nanofocusing by the use of plasmonic lens illuminated with radially polarized light, *Nano Lett.,* 9, 2139-2143(2009).
https://doi.org/10.1021/nl900694r

Hamazaki, J., Kawamoto, A., Morita, R. and Omasum, T., Direct production of high-power radially polarized output from a side-pumped Nd:YVO4 bounce amplifier using a photonic crystal mirror, *Opt. Express,* 16, 10762-10768(2008).
https://doi.org/10.1364/oe.16.010762

Hanming Guo, Xiaoyu Weng, Man Jiang, Yanhui Zhao, Guorong Sui, Qi Hu, Yang Wang and Songlin Zhuang, Tight focusing of a higher-order radially polarized beam transmitting through multi-zone binary phase pupil filters. *Opt. Express*, 21,5363-5372 (2013).
https://doi.org/10.1364/oe.21.005363

Helseth, L. E., Roles of polarization, phase and amplitude in solid immersion lens systems, *Opt. Commun.*, 191(3-6), 161-172(2001).
https://doi.org/10.1016/s0030-4018(01)01150-6

Homola, J., Sinclair S. Yee and Gauglitz, G., Surface plasmon resonance sensors: review, *Sensors and Actuat. B: Chem.,* 54(1-2), 3-15(1999).
https://doi.org/10.1016/s0925-4005(98)00321-9

Hu, Z. J., Tan, P. S., Zhu, S. W., and Yuan, X-C., Structured light for focusing surface plasmon polaritons, *Opt. Express*, 18(10), 10864-10870(2010).
https://doi.org/10.1364/oe.18.010864

Kozawa, Y. and Sato, S., Focusing property of a double-ring shaped radially polarized beam, *Opt. Lett.,* 31(6), 820-822(2006).
https://doi.org/10.1364/ol.31.000820

Kozawa, Y. and Sato, S., Generation of a radially polarized laser beam by use of a conical Brewster prism, *Opt. Lett.,* 30, 3063-3065(2005).

Kozawa, Y. and Sato, S., Sharper focal spot formed by higher-order radially polarized laser beams, *J. Opt. Soc. Am. A.,* 24(6), 1793-1798(2007).

Lalithambigai, K., Saraswathi, R. C., Anbarasan, P. M., Rajesh, K. B. and Jaroszewicz, Z., Generation of multiple focal hole segments using double-ring shaped azimuthally polarized beam, *J. At. Mol. Phys.,* 451715(2013).
https://doi.org/10.1155/2013/451715

Marcel Leutenegger, Ramachandra Rao, Rainer A. Leitgeb and Theo Lasser, Fast focus field calculations , *Opt. Express*, 14(23), 11277-11291(2006).
https://doi.org/10.1117/12.763188

Moh, K. J., Yuan, X. C., Bu, J., Zhu, S. W. amd Bruce Gao, Z., Surface plasmon resonance imaging of cell-substrate contacts with radially polarized beams, *Opt. Express.*, 16(25), 20734-20741(2008).

Moser, T., Glur, H., Romano, V., Pigeon, F., Parriaux, O., Ahmed, M. A. and Graf, T., Polarization-selective grating mirrors used in the generation of radial polarization, *Appl. Phys. B.,* 80(6), 707-713(2005).
https://doi.org/10.1007/s00340-005-1794-5

Qiwen Zhan, Evanescent Bessel beam generation via surface plasmon resonance excitation by a radially polarized beam, *Opt. Lett.*, 31(11), 1726-1728(2006).
https://doi.org/10.1364/OL.31.001726

Quabis, S., Dorn, R., Eberler, M., Glockl, O. and Leuchs, G., Focusing light to a tighter spot, *Opt. Commun.*, 179(1), 01-07(2000).
https://doi.org/10.1016/s0030-4018(99)00729-4

Rajesh, K.,B., Veerabagu Suresh, N., Anbarasan, P. M., Gokulakrishnan, K. *and Mahadevan,* G., Tight focusing of double ring shaped radially polarized beam with high NA lens axicon, *Opt. Laser., Tech.*, 43(7), 1037-1040(2011).
https://doi.org/10.1016/j.optlastec.2010.11.009

Richards, B. and Wolf, E., Electromagnetic diffraction in optical systems. II. Structure of the image field in an aplanatic system, *Proceedings of the Royal Society of London Series A*, 253(1274), 358-379(1959).
https://doi.org/10.1098/rspa.1959.0200

Sheppard, C. J. R. and Choudhury, A., Annular pupils, radial polarization and super resolution, *Appl. Opt.,* 43(22), 4322-4327(2004).
https://doi.org/10.1364/ao.43.004322

Tan, P. S., Yuan, X. C., Liu, J., Wang, Q., Mei, T., Burge, R. E. and Mu, G. G., Surface plasmon polaritons generated by optical vortex beams, *Appl. Phys. Lett.,* 92(11), 1108(2008).
https://doi.org/10.1063/1.2890058

Tian, B. and Pu, J., Tight focusing of a double-ring-shaped, azimuthally polarized beam, *Opt. Lett.,* 36(11), 2014-2016(2011).
https://doi.org/10.1364/ol.36.002014

Wenjun Gu, Zhehai Zhou, Qiaofeng Tan, Surface plasmon polaritions excitation by radially polarized vortex beams, *Proc. SPIE,* 8202(2011).
https://doi.org/10.1117/12.904899

Xin Jin, Hao Zhang, Yuchen Xu, Xiangchao Zhang, Heyuan Zhu, Representation and focusing properties of higher-order radially polarized Laguerre– aussian beams, *J. Mod. Opt.*, 62(8), 626-632(2015).
https://doi.org/10.1080/09500340.2014.999138

Youyi Zhuang, Yaoju Zhang, Biaofeng Ding, Taikei Suyama, Trapping rayleigh particles using highly focused higher-order radially polarized beams, *Opt, Commun.,* 284(7), 1734-1739(2011).
https://doi.org/10.1016/j.optcom.2010.12.018

Zhan, Q., Cylindrical vector beams: from mathematical concepts to applications, *Adv. Opt. Photonics.,* 1(1), 01-57(2009).
https://doi.org/10.1364/aop.1.000001

Zhang, Z., Pu, J. and Wang, X., Tightly focusing of linearly polarized vortex beams through a dielectric interface, *Opt. Commun.*, 281(13), 3421-3426 (2008). https://doi.org/10.1016/j.optcom.2008.03.043

Zhang, Y. and Bai, J., Improving the recording ability of a near-field optical storage system by higher-order radially polarized beams, *Opt. Express*., 17(5), 3699-3706(2009).
https://doi.org/10.1364/oe.17.003698

Zhongsheng Man, Luping Du, Changjun Min, Yuquan Zhang, Chonglei Zhang, Siwei Zhu, Paul Urbach, H. and Yuan, X.-C., Dynamic plasmonic beam shaping by vector beams with arbitrary locally linear polarization states, *Appl. Phys. Lett.,* 105(1), 011110(2014).
https://doi.org/10.1063/1.4887824

Zhongsheng Man, Wei Shi, Yuquan Zhang, Chonglei Zhang, Changjun Min, Yuan, X-C., Properties of surface plasmon polaritons excited by generalized cylindrical vector beams, *Appl. Phys. B.,* 119, 305-311(2015).
https://doi.org/10.1007/s00340-015-6064-6